Science and Technology for the Built Environment

ISSN: 2374-4731 (Print) 2374-474X (Online) Journal homepage: https://www.tandfonline.com/loi/uhvc21

Normal and extreme aircraft accelerations and the effects on exposure to expiratory airborne contaminant inside commercial aircraft cabins

A technical note in response to: "Are aircraft acceleration-induced body forces effective on contaminant dispersion in passenger aircraft cabins?" and "Airflow design and source control strategies for reducing airborne contaminant exposure in passenger aircraft cabins during the climb leg" (2019) in Sci. Technol. Built En.

Hossam A. Elmaghraby, Yi Wai Chiang & Amir A. Aliabadi

To cite this article: Hossam A. Elmaghraby, Yi Wai Chiang & Amir A. Aliabadi (2020) Normal and extreme aircraft accelerations and the effects on exposure to expiratory airborne contaminant inside commercial aircraft cabins , Science and Technology for the Built Environment, 26:7, 924-927, DOI: 10.1080/23744731.2020.1771808

To link to this article: https://doi.org/10.1080/23744731.2020.1771808

Accepted author version posted online: 19 May 2020.
Published online: 04 Jun 2020.

Science and Technology for the Built Environment, (2020) **26**, 924–927

ISSN: 2374-4731 print / 2374-474X online
DOI: 10.1080/23744731.2020.1771808

Normal and extreme aircraft accelerations and the effects on exposure to expiratory airborne contaminant inside commercial aircraft cabins

A technical note in response to: "Are aircraft acceleration-induced body forces effective on contaminant dispersion in passenger aircraft cabins?" and "Airflow design and source control strategies for reducing airborne contaminant exposure in passenger aircraft cabins during the climb leg" (2019) in Sci. Technol. Built En.

HOSSAM A. ELMAGHRABY, YI WAI CHIANG, AND AMIR A. ALIABADI*

School of Engineering, University of Guelph, RICH 2515, Guelph, ON N1G 2W1, Canada

A novel dataset based on satellite observations of aircraft positions was utilized to estimate normal accelerations of commercial aircraft during climb and descent legs. Further, these accelerations are used to simulate the effects on exposure to expiratory airborne contaminant inside commercial aircraft cabins. Compared to previous studies, which reported exposures more than twice due to high aircraft accelerations during the climb leg, the new findings suggest lower aircraft accelerations that result in exposures on par with steady level flights during climb and descent legs. The new findings place previous studies in context to be interpreted as extreme conditions only while they call for more detailed experimental investigations.

Introduction

The articles (Elmaghraby, Chiang, and Aliabadi 2019a, 2019b) used an analytical method based on Newton's second law to estimate commercial aircraft accelerations during climb and descent legs for a Boeing 767 passenger aircraft. Those acceleration values were further used to investigate the effects on exposure to expiratory airborne contaminant inside commercial aircraft cabins. It was found that due to acceleration-induced body forces the exposure ratios could more than double during the climb leg compared to steady flight conditions.

A new data source became available to the authors of this letter that provides an alternative approach to determine commercial aircraft accelerations during climb and descent legs based on satellite observation of aircraft positions. This method results in new estimates of exposure to expiratory airborne contaminant inside commercial aircraft cabins based on simulations. The authors have repeated identical simulations as were performed by the authors of the articles (Elmaghraby, Chiang, and Aliabadi 2019a, 2019b), except for changing aircraft accelerations to the newly observed accelerations. The results predict lower exposures under "normal" climb and descent using observed accelerations that place the findings of (Elmaghraby, Chiang, and Aliabadi 2019a, 2019b) in context to be interpreted as "extreme" conditions only.

The method used to attain the "normal" acceleration components during the climb and descent legs serves as an alternative method to the calculations conducted using Newton's second law $\left(\sum \vec{F} = m\vec{a}\right)$. This is because the latter calculation method lacks enough actual field measurements to support it, and led the authors to quantify and use "extreme" values for the acceleration components during the climb and descent legs that do not occur under the "normal" operating conditions of the commercial aircraft. However, those high acceleration values can still be applied to the aircraft operating under "extreme" operating conditions whose details are described below.

Methods

The alternative method utilizes actual commercial aircraft traffic satellite data extracted from the U.S. National

Received July 11, 2019; Accepted May 15, 2020
Hossam A. Elmaghraby, PhD., is a Postdoctoral Fellow. **Yi Wai Chiang, Ph.D., P.Eng.,** is an Assistant Professor. **Amir A. Aliabadi, Ph.D., P.Eng.,** is an Assistant Professor.
*Corresponding author e-mail: aliabadi@uoguelph.ca

Oceanic and Atmospheric Administration (NOAA) website, and more specifically their Aircraft Meteorological Data Relay (AMDAR) satellite system (NOAA. 2019). The AMDAR satellite system data has been successfully used by Zhang et al. (2019) for investigation of the diurnal variation of Planetary Boundary Layer (PBL) physical characteristics.

The elevation, latitude, and longitude data for one hundred different aircraft, fifty for climb and fifty for descent, was extracted from NOAA and processed to produce the vertical and horizontal acceleration components during each flight leg. This was made possible by conducting second order curve-fitting (regression) for each aircraft dataset (versus time) and finding the acceleration components using a Python code according to the following equation representing the kinematic equation of motion:

$$d = at^2 + bt + c, \tag{1}$$

where d is distance traveled from the origin (vertically or horizontally), t is the time, and a, b, and c are constants. Also, the constant $a = {}^1\!/_2\, a_c$ is related to the average acceleration during the analyzed time of motion, where a_c is either the average vertical (a_v) or average horizontal (a_h) acceleration components.

Figure 1 shows the distribution of acceleration components for each of the fifty aircraft during climb and fifty aircraft during the descent legs. The analyzed time of motion is 350 s. This time span was used in order to yield representative solutions for the airflow velocity and contaminant dispersion fields without imposing excessive computational burden. This is also inspired by other studies in the literature that used a similar time span for their aerosol dispersion analyses (Sze To et al. 2009; Wan et al. 2009).

The chosen values for the vertical and horizontal acceleration components used in the climb and descent simulations were taken as the mean values for the fifty aircraft for each type of flight leg (climb or descent). Those average accelerations (also shown in Figure 1) in addition to the median and standard deviation values are shown in Table 1. Note that the gravitational acceleration is removed from these estimates. The signs of the acceleration components represent their direction with respect to the set axes mentioned in Elmaghraby, Chiang, and Aliabadi (2019a, 2019b).

Results and discussion

Two simulations were run; one for the climb case and the other for the descent, using the calculated acceleration components. The resulting concentration time series of the SF_6 contaminant surrogate in the cabin for the climb and descent legs from the simulations using those acceleration values are referred to as "aircraft normal operating conditions". On the other hand, the SF_6 concentration time series predicted using the accelerations calculated from Newton's second law in Elmaghraby, Chiang, and Aliabadi (2019a, 2019b), which reached a maximum of 1.4 g (excluding gravitational acceleration) in the vertical direction, are considered to occur under "extreme aircraft operating conditions". The extreme

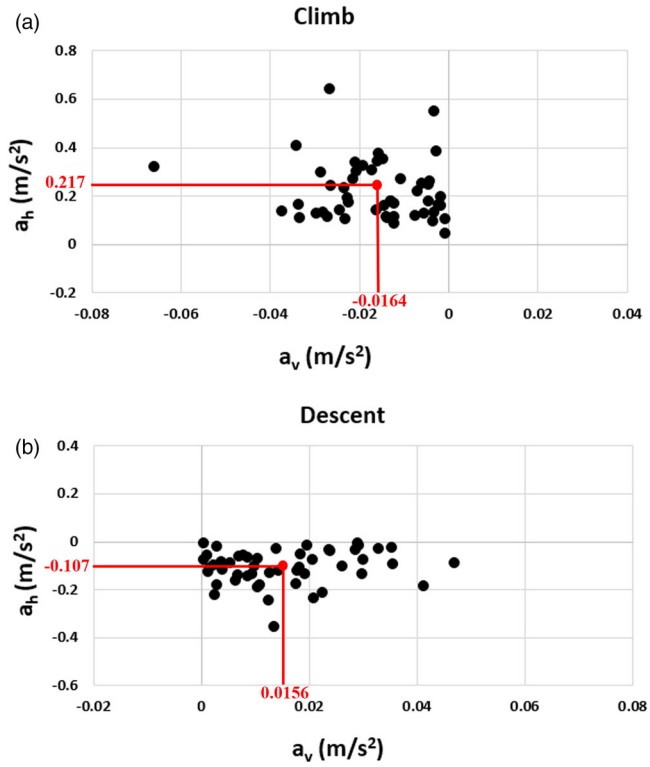

Figure 1. The quantified vertical (a_v) and horizontal (a_h) acceleration components from second order regression of data from fifty different aircraft flights; (a) during climb, and (b) during descent.

accelerations are still realistic based on the U.S. Federal Aviation Administration (FAA) regulations that consider that the acceleration components with a maximum of 1.4 g (excluding gravitational acceleration) are possible during extreme events of turbulence, gusts, maneuvers, and turns. Moreover, those acceleration values are within the safe limits for commercial aircraft structures given that they occur for limited time periods (U.S. Federal Aviation Administration (FAA)) 2016). Figures 2 and 3 depict comparisons of the SF_6 concentration time series in the simulated aircraft cabin model among the baseline steady level flight case and the climb and descent cases under the "normal" and "extreme" aircraft operating conditions.

From Figure 2, it can be noticed that the SF_6 concentration is considerably higher at the two monitoring locations, seat A7 and seat C7, for the climb under the extreme operating conditions as compared to the normal conditions. However, the concentration for the climb under the normal conditions is comparable to that during the steady level flight case with the peak concentration noticed to be higher for the steady level flight case at the two locations. This is especially evident at seat C7, at which the peak SF_6 concentration for the normal climb is reduced by about 50% from the steady level flight case.

On the other hand, from Figure 3, the SF_6 concentration time series during descent under normal conditions is different between the two locations when compared to that for the descent under extreme conditions and the steady level flight

Table 1. Mean, median, and standard deviation for the aircraft vertical and horizontal acceleration values during normal climb and descent.

Case	Acceleration Component / Value [m s^{-2}]		
Climb (Normal Conditions)	Vertical Component	Mean	−0.0164
		Median	−0.0145
		Standard Deviation	0.0125
	Horizontal Component	Mean	0.217
		Median	0.178
		Standard Deviation	0.119
Descent (Normal Conditions)	Vertical Component	Mean	0.0156
		Median	0.0132
		Standard Deviation	0.0118
	Horizontal Component	Mean	−0.108
		Median	−0.0998
		Standard Deviation	0.0723

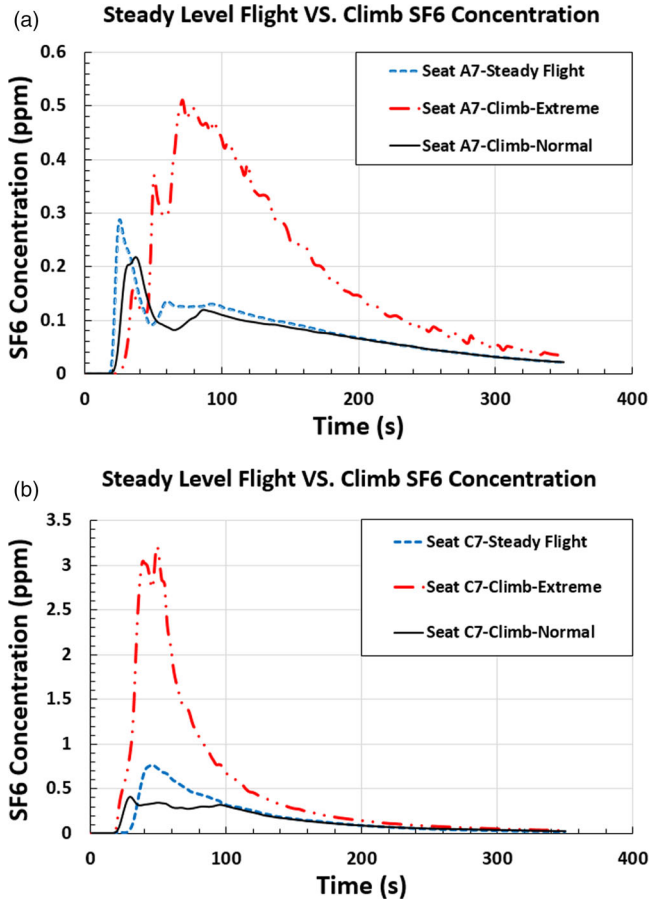

Figure 2. Comparison of the predicted SF_6 concentration time series between the steady level flight case and the climb case under the normal and extreme aircraft operating conditions; (a) at seat A7, and (b) at seat C7.

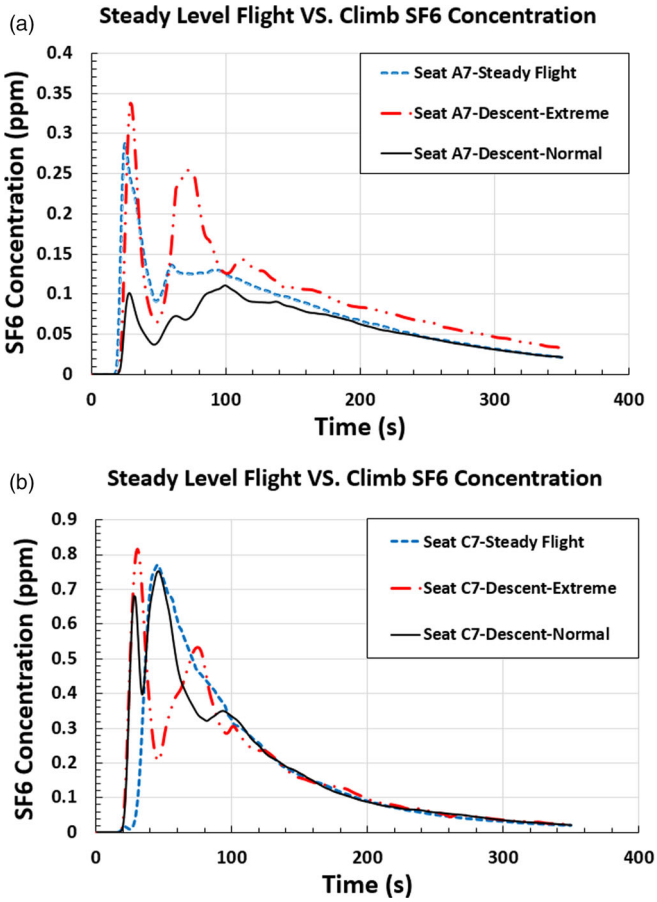

Figure 3. Comparison of the predicted SF_6 concentration time series between the steady level flight case and the descent case under the normal and extreme aircraft operating conditions; (a) at seat A7, and (b) at seat C7.

cases. At seat A7, the SF_6 concentration during normal conditions descent is noticeably less than its counterparts for the extreme conditions' descent and steady level flight cases. At seat C7, however, the normal conditions descent's SF_6 concentration time series is almost identical to that for the extreme conditions' descent and steady level flight scenarios.

To put the comparisons into numerical figures, Table 2 lists the passenger exposure ratios of the climb and descent cases under the extreme and normal operating conditions to

Table 2. Ratio of passenger exposure between climb and descent cases under extreme and normal operating conditions and the baseline steady level flight case at the two monitoring locations: seat A7 and seat C7.

	Passenger Exposure Ratio to Baseline Steady Level Flight Case	
Case	Seat A7	Seat C7
Climb (Extreme Conditions)	2.4 : 1	2.8 : 1
Climb (Normal Conditions)	0.92 : 1	0.77 : 1
Descent (Extreme Conditions)	1.3 : 1	0.93 : 1
Descent (Normal Conditions)	0.75 : 1	0.99 : 1

the baseline steady level flight case. The passenger exposures are estimated by calculating the area under each concentration time series curve according to the following equation:

$$Exposure = \int_0^{350\ s} C_{SF_6}(t)\ dt. \quad (2)$$

From Table 2, the calculated passenger exposure ratios agree well with the graphical representation for the SF_6 concentration time series in Figures 2 and 3.

Conclusions

The results show that the simulated passenger exposure ratios to baseline steady level conditions are very sensitive to the climb and descent leg accelerations calculated. Although there are uncertainties in any estimate of commercial aircraft accelerations during the climb and descent legs, the new satellite-based data system enabled the calculation of aircraft accelerations closer to normal conditions. The new findings place previous studies by Elmaghraby, Chiang, and Aliabadi (2019a, 2019b) in context so that the exposure ratios reported previously are only to be interpreted as "extreme" case exposure while exposure ratios under "normal" conditions can be less. Finally, the findings in this technical note call for more detailed experimental studies to quantify aircraft accelerations and their effects on airborne contaminant dispersion inside aircraft cabins under realistic conditions. To the best of authors' knowledge, the subject has rarely been studied in the literature and requires more investigations.

Funding

This work was supported by the Discovery Grant program (401231) from the Natural Sciences and Engineering Research Council (NSERC) of Canada.

ORCID

Hossam A. Elmaghraby http://orcid.org/0000-0002-8613-6958
Yi Wai Chiang http://orcid.org/0000-0002-7798-9166
Amir A. Aliabadi http://orcid.org/0000-0002-1002-7536

References

Elmaghraby, H. A., Y. W. Chiang, and A. A. Aliabadi. 2019a. Are aircraft acceleration-induced body forces effective on contaminant dispersion in passenger aircraft cabins? *Science and Technology for the Built Environment* 25 (7):858–872. doi:10.1080/23744731.2019.1576457

Elmaghraby, H. A., Y. W. Chiang, and A. A. Aliabadi. 2019b. Airflow design and source control strategies for reducing airborne contaminant exposure in passenger aircraft cabins during the climb leg. *Science and Technology for the Built Environment*: 1–23. doi:10.1080/23744731.2019.1634930

NOAA. 2019. NOAA AMDAR data display. https://amdar.noaa.gov/, last Accessed May 23, 2020.

Sze To, G. N., M. P. Wan, C. Y. H. Chao, L. Fang, and A. Melikov. 2009. Experimental study of dispersion and deposition of expiratory aerosols in aircraft cabins and impact on infectious disease transmission. *Aerosol Science and Technology* 43 (5): 466–485. doi:10.1080/02786820902736658

U.S. Federal Aviation Administration (FAA). 2016. *Pilot's Handbook of Aeronautical Knowledge.* Oklahoma, OK: U.S. Department of Transportation, Federal Aviation Administration.

Wan, M. P., G. N. Sze To, C. Y. H. Chao, L. Fang, and A. Melikov. 2009. Modeling the fate of expiratory aerosols and the associated infection risk in an aircraft cabin environment. *Aerosol Science and Technology* 43 (4):322–343. doi:10.1080/02786820802641461

Zhang, Y., D. Li, Z. Lin, J. A. Santanello Jr, and Z. Gao. 2019. Development and evaluation of a long-term data record of planetary boundary layer profiles from aircraft meteorological reports. *Journal of Geophysical Research: Atmospheres* 124 (4): 2008–2030. doi:10.1029/2018JD029529